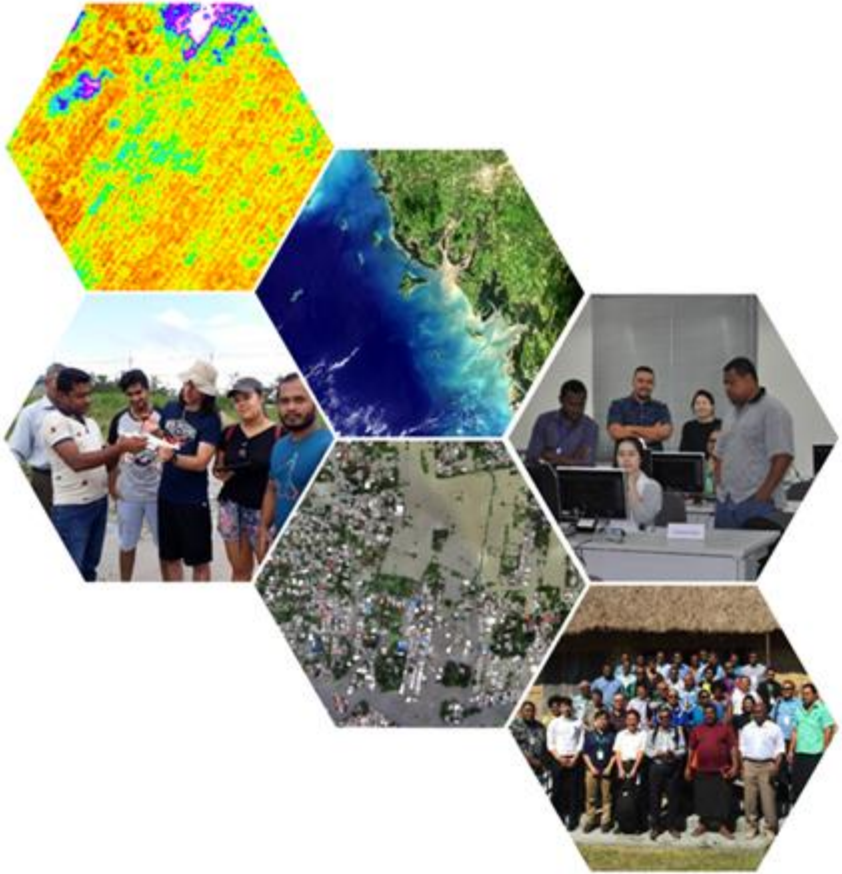

Flood Detection and Mapping using RS Data

syams@ait.asia

Geoinformatics Center - AIT

Remote Sensing for Flood Mapping

Both active and passive sensors onboard different satellites are being extensively used for water segmentation and flood mapping.

- Assist with large-scale and extensive flood phenomena
- Provide near-real-time monitoring
- Multiple remote sensing sensors provide various types of valuable data
- Historical record and change detection
- Cost-effectiveness

Remote Sensing for Flood Mapping

Flood mapping in Central Java, Indonesia, using ALOS-2 L-band SAR data

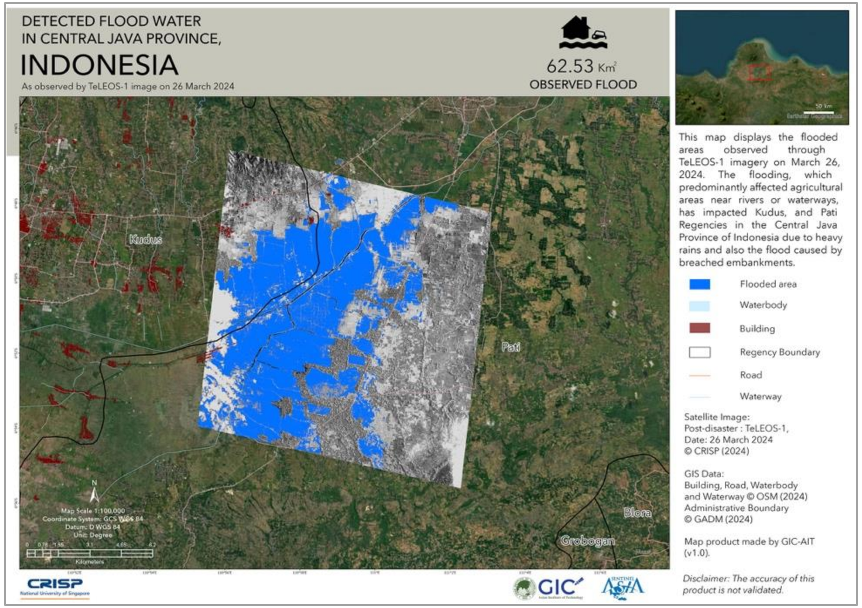

Flood mapping in Central Java, Indonesia, using 1m TelEOS-1 optical data

Remote Sensing for Flood Mapping

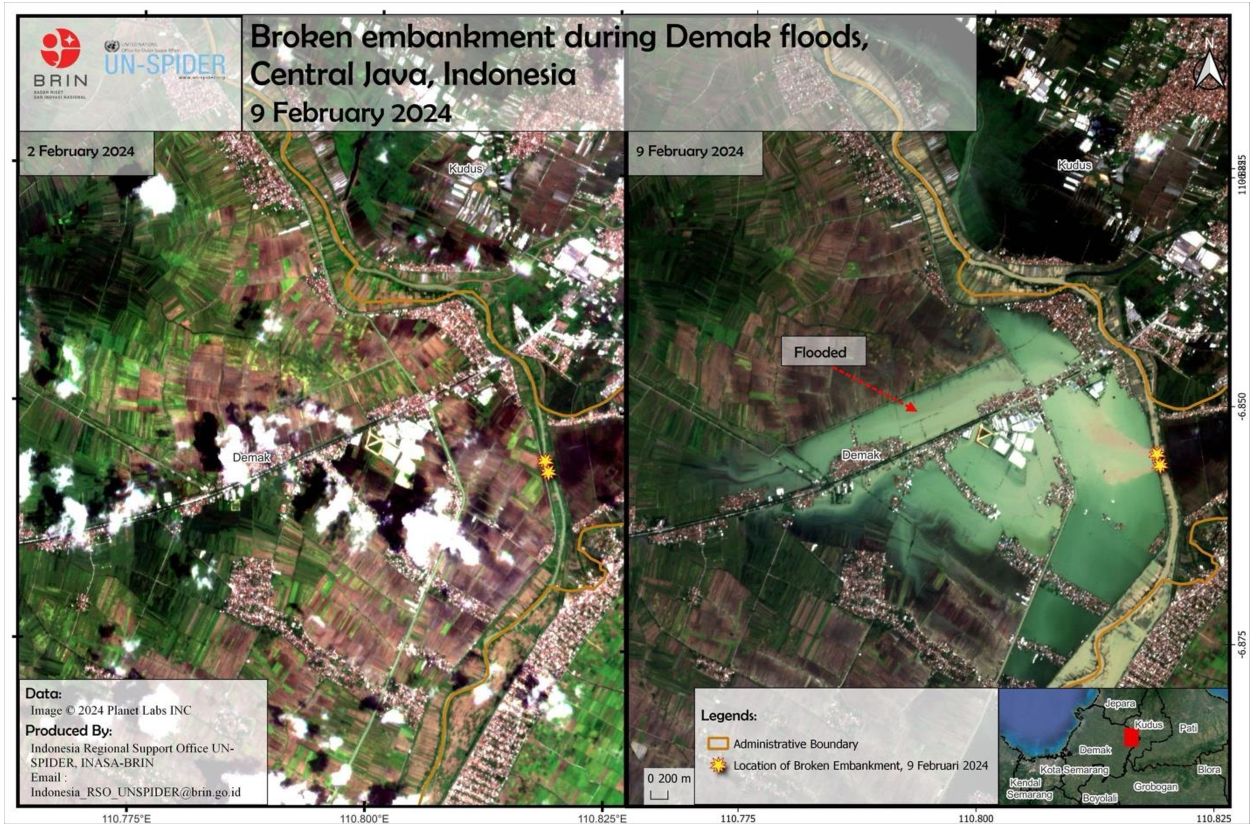

Flood mapping and detection of broken embankment in Central Java, Indonesia, using Planet Labs optical data

Remote Sensing for Flood Mapping

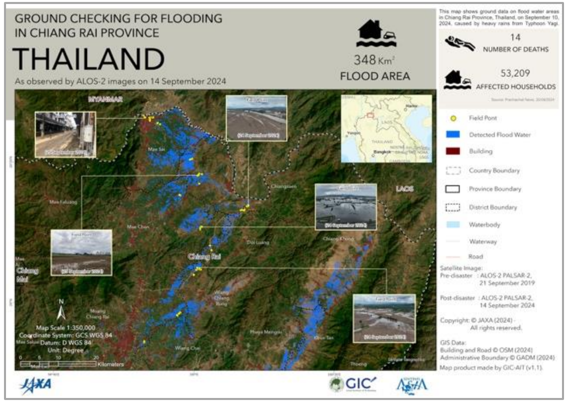

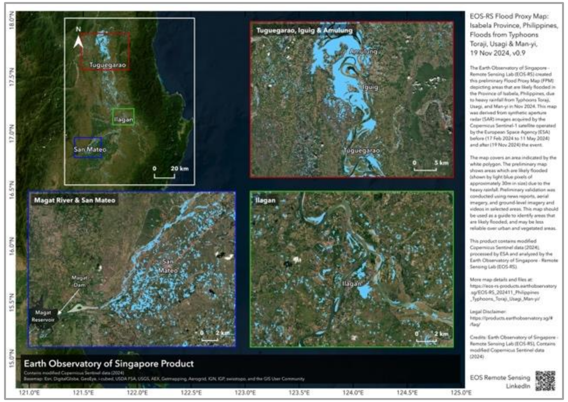

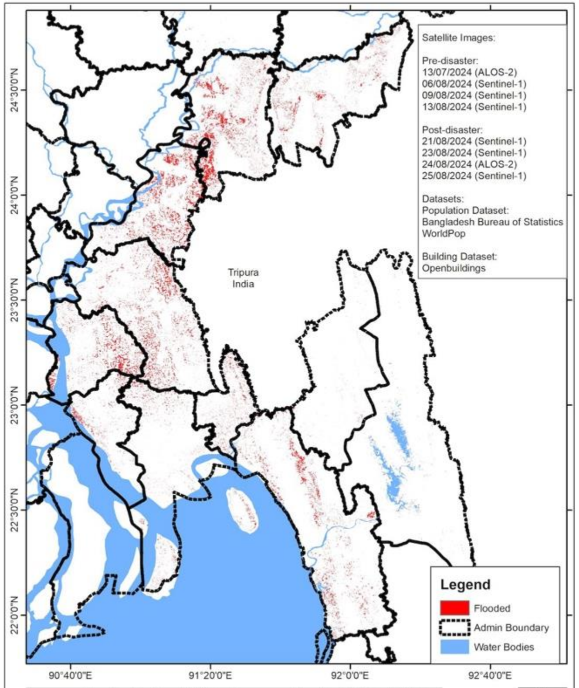

District	Inundated Area (sq-km)	Affected Population	Affected Buildings	District	Inundated Area (sq-km)	Affected Population	Affected Buildings
Bramanbaria	271	308643	2691	Khagrachari	10	2449	25
Chandpur	160	120117	1476	Laxmipur	59	57047	653
Chittagong	219	149784	2400	Moluvibazar	66	19199	146
Comilla	247	247154	2533	Noakhali	70	61661	908
Feni	54	71844	1116	Rangamati	62	1511	176
Habiganj	291	247545	1411	Total	1509	1286954	13535

(Disclaimer: The accuracy of the product has not been validated)

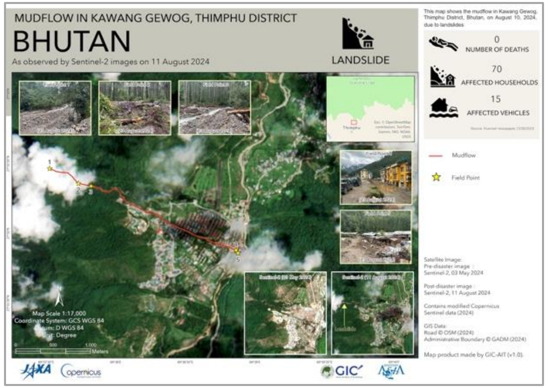

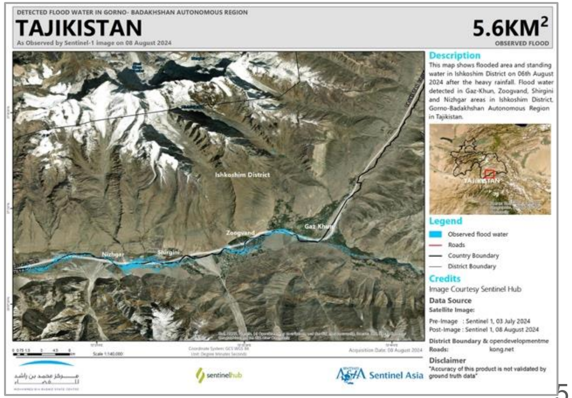

Remote Sensing for Flood Mapping

Historic milestones in satellite remote sensing of floods.

Breakthrough/Milestone event	Satellite/Sensor	Year[a]	Progress enabled	Barrier lifted
MS1: The first flood map	Landsat-1	1973	Flood mapping from space demonstrated	Beyond small scale mapping
MS2: Seeing through clouds	SIR-B	1984	All-weather, day and night capability demonstrated	Restricted to good weather and sunlight
MS3: Disaster Charter	Interagency satellite tasking	2000	State-of-the-art international collaboration enabling free multi-mission satellite tasking	Difficulty in satellite tasking during disasters
MS4: Global mapping potential	MODIS Terra/Aqua	2003	Sub-daily revisit time	Capturing a much larger number of flood events
MS5: Copernicus programme	Sentinel-1	2014	Open-access operational satellite data	Beyond free opportunistic SAR satellite data
MS6: WorldFloods	Wild Ride	2019	Machine learning-based flood mapping onboard optical satellite	Latency in flood map delivery

[a]Denotes year of flood-relevant breakthrough, not year of launch of satellite or sensor.

J-P. Schumann, Guy. “Breakthroughs in Satellite Remote Sensing of Floods.” *Frontiers in Remote Sensing* 4 (April 29, 2024). https://doi.org/10.3389/frsen.2023.1280654.

Types of Floods

River floods

- caused by extensive precipitation over long periods, causing the river to overflow its banks, ultimately inundating the neighboring areas.
- this process is slow and can last for several days.

Flash floods

- caused by short but intense rainfall or sudden melting of snow.
- rapid and intense floods, typical of mountain and steep catchments.
- usually coupled with other hazards such as debris flows and landslides.

Coastal floods

- caused by extreme meteorological conditions which increase the water level in large bodies of water, due to a combination of low atmospheric pressure and strong winds.
- occur near oceans, seas, or large lakes.

Floods in in the Yangtze River, China (Caixin Global, July 2, 2024)

Flash Flood in Puncak Bogor Sweeps Away Resident, Triggers Landslide (Tempo, March 2, 2025)

Types of Floods

Urban floods

- caused by the failure of drainage from a sewer system, due to extreme precipitation, resulting in the overflow of those pipes.
- depending on the city position and topography, these floods can also be affected by all the other types of floods.

Dam break and dike breach floods

- caused by the failure of flood protection structures, due to extreme flood events or management issues.

Annual Flooding in in Jakarta, Indonesia (January 2013)

Flooding at the Ratchada-Lat Phrao intersection, Bangkok, Thailand (Bangkok Post, May 19, 2022)

What are we mapping?

- water extent =

The total area covered by water at a certain point in time (derived from e.g. post-disaster data)
bright blue and blue

- normal water level =

The total area covered by water during the average water level conditions (derived from pre-disaster archive data)
blue

- flood extent =

(total) water extent minus normal water level (requires pre- and post-disaster data)
bright blue

Flood Detection using Optical Data

Advantages:

- The availability of several spectral bands with different wavelengths, makes it possible to derive valuable information from each band and surfaces' spectral signatures,
- With simple math algebra, remote sensing indices exploit the reflectance characteristics of different objects.
- Direct interpretation of true- and false-color composites.

Disadvantages:

- Cloud cover affects optical sensors
- High-resolution data can be expensive
- Need for ground validation in some cases

Flood Detection using Optical Data

Methodologies applied to detect flooded areas using optical data:

- Multispectral indices for water and floodwater - thresholding.
- Supervised classification: maximum likelihood, decision tree, random forest, support vector machine, neural network and deep learning
- Unsupervised approaches: ISODATA clustering
- Sub-pixel techniques

Flood Detection using Optical Data

Main spectral and spatial resolution characteristics of the selected satellites commonly used in water detection methods

	Landsat 4- , 5-TM			Landsat 7-ETM+			Landsat 8-OLI			Sentinel-2 MSI			Terra–Aqua MODIS		
Band	**Band Number**	**W (μm)**	**R (m)**	**Band Number**	**W (μm)**	**R (m)**	**Band Number**	**W (μm)**	**R (m)**	**Band Number**	**W (μm)**	**R (m)**	**Band Number**	**W (μm)**	**R (m)**
Blue	Band 1	0.45–0.52	30	Band 1	0.45–0.52	30	Band 2	0.45–0.51	30	Band 2	0.46–0.52	10	Band 3	0.46–0.48	500
Green	Band 2	0.52–0.60	30	Band 2	0.52–0.60	30	Band 3	0.53–0.59	30	Band 3	0.55–0.58	10	Band 4	0.55–0.57	500
Red	Band 3	0.63–0.69	30	Band 3	0.63–0.69	30	Band 4	0.64–0.67	30	Band 4	0.64–0.67	10	Band 1	0.62–0.67	250
NIR	Band 4	0.76–0.90	30	Band 4	0.77–0.90	30	Band 5	0.85–0.88	30	Band 8	0.78–0.90	10	NIR 1 Band 2	0.84–0.88	250
													NIR 2 Band 5	1.23–1.25	500
SWIR 1	Band 5	1.55–1.75	30	Band 5	1.55–1.75	30	Band 6	1.57–1.65	30	Band 11	1.57–1.65	20	Band 6	1.63–1.65	500
SWIR 2	Band 7	2.08–2.35	30	Band 7	2.09–2.35	30	Band 7	2.11–2.29	30	Band 12	2.10–2.28	20	Band 7	2.11–2.16	500
Data Access	USGS EarthExplorer data portal [36] https://earthexplorer.usgs.gov/ (accessed on 4 February 2022)									Sentinel Scientific Data Hub [37] https://scihub.copernicus.eu/ (accessed on 4 February 2022)			USGS EarthExplorer data portal [36] https://earthexplorer.usgs.gov/ (accessed on 4 February 2022) NASA Earthdata Search [38] https://search.earthdata.nasa.gov/search (accessed on 4 February 2022) LAADS DAAC Archive [39] https://ladsweb.modaps.eosdis.nasa.gov/ (accessed on 4 February 2022)		

Albertini, et al. “Detection of Surface Water and Floods with Multispectral Satellites.” *Remote Sensing* 14, no. 23 (January 2022): 6005. https://doi.org/10.3390/rs14236005.

Flood Detection using Optical Data

Multispectral Indices for Water Segmentation

Index Formula		NDVI	NDWI	NDMI	MNDWI	WRI	MNDWI7
	Reference	Rouse et al. [33]	McFeeters [34]	Gao [104]	Xu [26]	Shen and Li [107]	Ji et al. [106]
		$\frac{NIR-RED}{NIR+RED}$	$\frac{GREEN-NIR}{GREEN+NIR}$	$\frac{NIR-SWIR\ 1}{NIR+SWIR\ 1}$	$\frac{GREEN-SWIR\ 1}{GREEN+SWIR\ 1}$	$\frac{GREEN+RED}{NIR+SWIR\ 1}$	$\frac{GREEN-SWIR\ 2}{GREEN+SWIR\ 2}$
	Landsat 5-TM 7-ETM+	$\frac{B4-B3}{B4+B3}$	$\frac{B2-B1}{B2+B1}$	$\frac{B4-B5}{B4+B5}$	$\frac{B2-B5}{B2+B5}$	$\frac{B2+B3}{B4+B5}$	$\frac{B2-B7}{B2+B7}$
	Landsat 8-OLI	$\frac{B5-B4}{B5+B4}$	$\frac{B3-B5}{B3+B5}$	$\frac{B5-B6}{B5+B6}$	$\frac{B3-B6}{B3+B6}$	$\frac{B3+B4}{B5+B6}$	$\frac{B3-B7}{B3+B7}$
	Sentinel-2 MSI	$\frac{B8-B4}{B8+B4}$	$\frac{B3-B8}{B3+B8}$	$\frac{B8-B11}{B8+B11}$	$\frac{B3-B11}{B3+B11}$	$\frac{B3+B4}{B8+B11}$	$\frac{B3-B12}{B3+B12}$
	Terra–Aqua MODIS	$\frac{B2-B4}{B2+B4}$	$\frac{B4-B2}{B4+B2}$	$\frac{B2-B5}{B2+B5}$	$\frac{B4-B6}{B4+B6}$	$\frac{B4+B1}{B2+B6}$	$\frac{B4-B7}{B4+B7}$

Albertini, et al. “Detection of Surface Water and Floods with Multispectral Satellites.” *Remote Sensing* 14, no. 23 (January 2022): 6005. https://doi.org/10.3390/rs14236005.

Flood Detection using Optical Data

Multispectral Indices for Water Segmentation

		AWEInsh	AWEIsh
	Reference	Feyisa et al. [105]	Feyisa et al. [105]
Index Formula		$4 \cdot (GREEN - SWIR\,1) - 0.25 \cdot (NIR + 2.75 \cdot SWIR\,2)$	$BLUE + 2.5 \cdot GREEN - 1.5 \cdot (NIR + SWIR\,1) - 0.25 \cdot SWIR\,2$
	Landsat 5-TM 7-ETM+	$4 \cdot (B2 - B5) - 0.25 \cdot (B4 + 2.75 \cdot B7)$	$B1 + 2.5 \cdot B2 - 1.5 \cdot (B4 + B5) - 0.25 \cdot B7$
	Landsat 8-OLI	$4 \cdot (B3 - B6) - 0.25 \cdot (B5 + 2.75 \cdot B7)$	$B2 + 2.5 \cdot B3 - 1.5 \cdot (B5 + B6) - 0.25 \cdot B7$
	Sentinel-2 MSI	$4 \cdot (B3 - B11) - 0.25 \cdot (B8 + 2.75 \cdot B12)$	$B2 + 2.5 \cdot B3 - 1.5 \cdot (B8 + B11) - 0.25 \cdot B12$
	Terra–Aqua MODIS	$4 \cdot (B4 - B6) - 0.25 \cdot (B2 + 2.75 \cdot B7)$	$B3 + 2.5 \cdot B4 - 1.5 \cdot (B2 + B6) - 0.25 \cdot B7$

Albertini, et al. "Detection of Surface Water and Floods with Multispectral Satellites." *Remote Sensing* 14, no. 23 (January 2022): 6005. https://doi.org/10.3390/rs14236005.

Flood Detection using SAR Data

Advantages:

- Reliable data collection during flood events: weather independence, cloud-free data, day and night operation.
- Strong contrast between water and land
- Data availability (TerraSAR-X, Cosmo-SkyMed, ALOS-2, Radarsat-2, ...)
- Spatial resolution, repetition rate

Disadvantages:

- Speckle noise affects image quality
- Complex data processing required
- Signal confusion in urban areas
- False detection from smooth surfaces

Flood Detection using SAR Data

How does Synthetic Aperture Radar (SAR) detect floods?

- Water (calm) surface appears dark due to specular reflection leading to low backscatter.
- Non-water (Land) surface appear brighter due to the rough surface leading to higher backscatter.

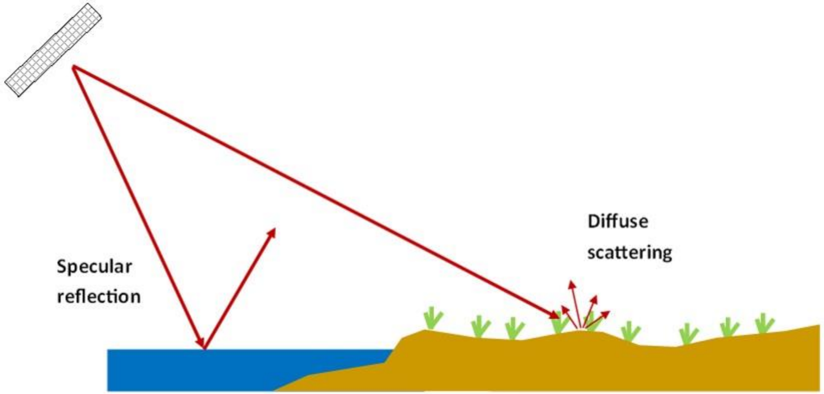

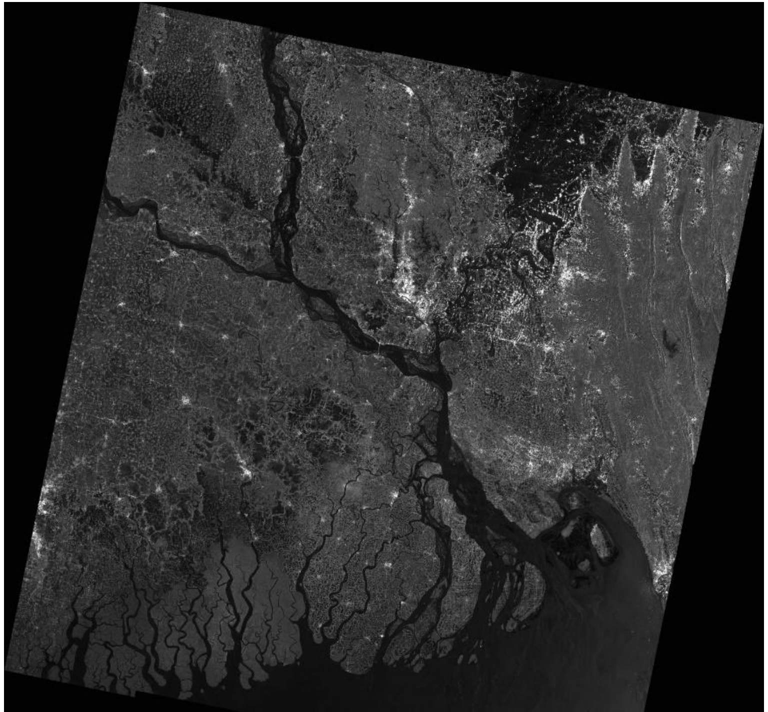

Bangladesh floods observed by ALOS-2 Level2.1
IMG HH ALOS2 43575/3150 2022/06/18 WBD R 2.1 GUD

Flood Detection using SAR Data

Surface Water Signatures in SAR Amplitude Images

Waterbody mapping from SAR data is based on:

- **Unique sensitivity to variations in soil moisture** and presence/absence of surface water or water under vegetation
- **Specular reflection at standing surface water patches** → dark backscatter
- In vegetated areas:
  - Long wavelengths preferable due to better penetration of vegetation cover
  - Enhanced return if tree cover underlain by water (double bounce effect – smooth water surface – vertical vegetation structures)
  - Enhanced backscatter for wet soils

Flood Detection using SAR Data

1. Open Lands – Areas with Low Vegetation Cover

Waterbody mapping from SAR data is based on:

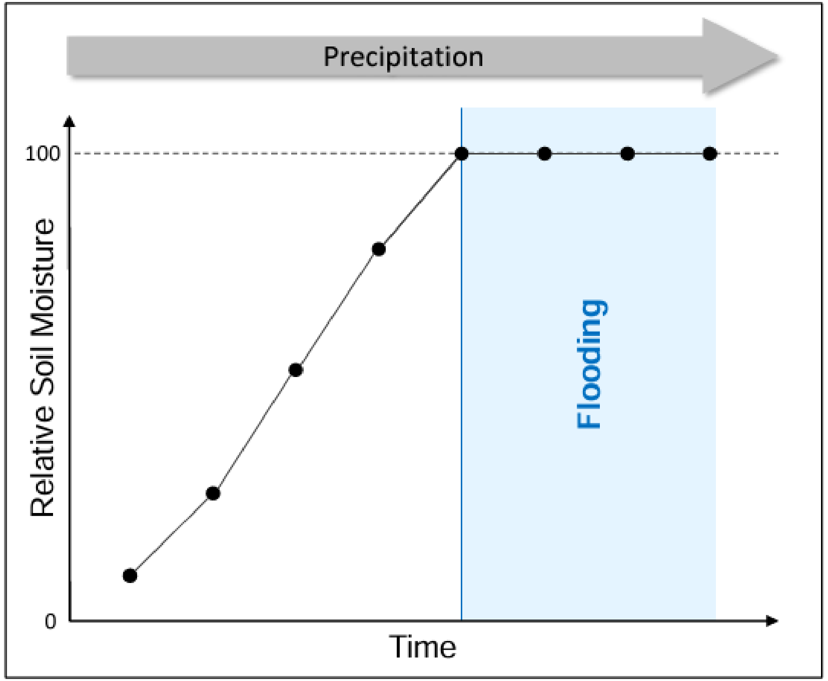

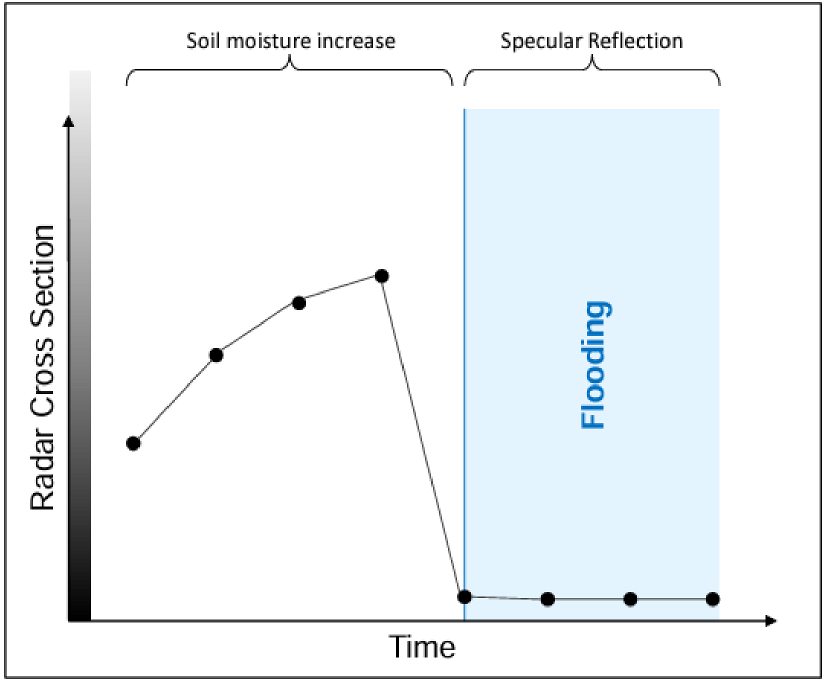

Flood Detection using SAR Data

2. Flooding under Vegetation Canopies

Mapping inundation under vegetation canopies::

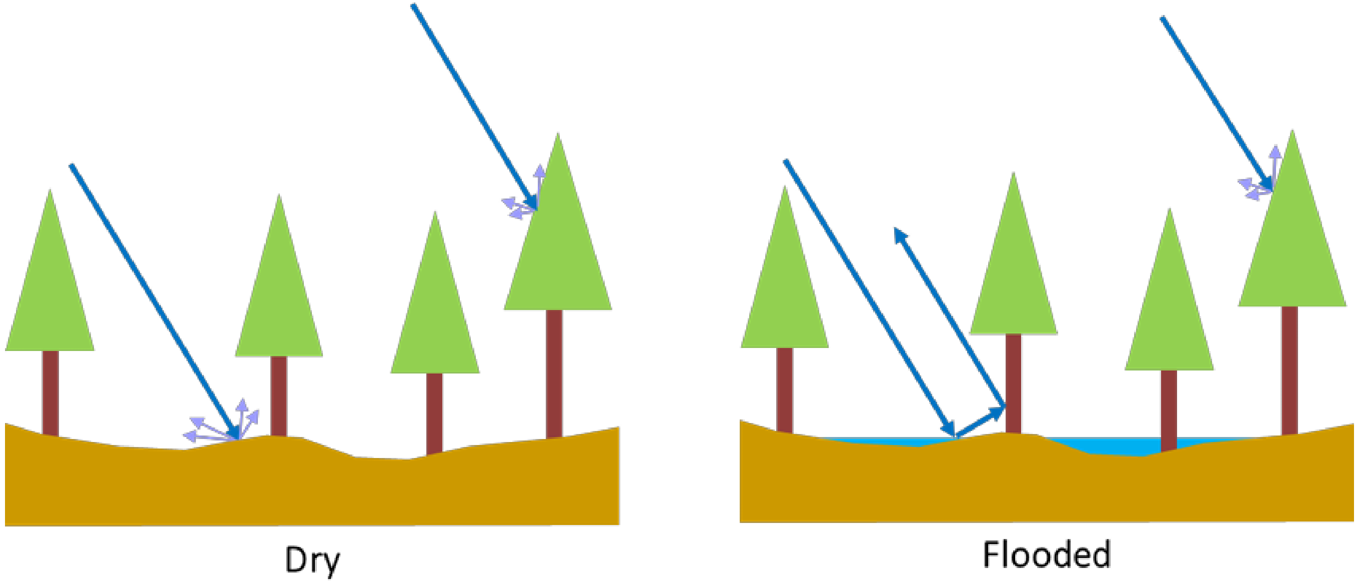

Enhanced return if tree cover is underlain by water (double bounce effect – smooth water surface – vertical vegetation structures)

Flood Detection using SAR Data

2. Flooding under Vegetation Canopies

Relative SAR response in vegetated canopies as precipitation increases::

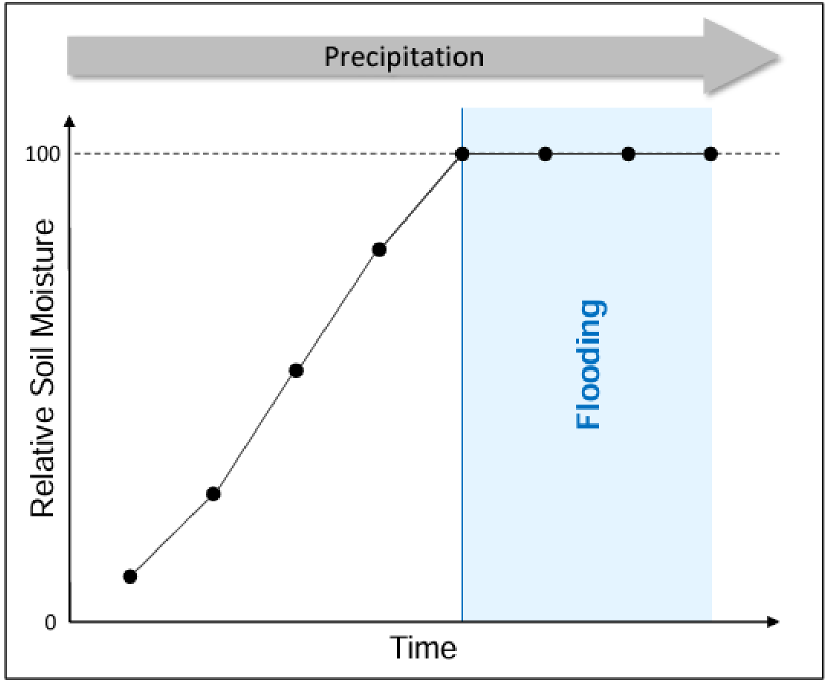

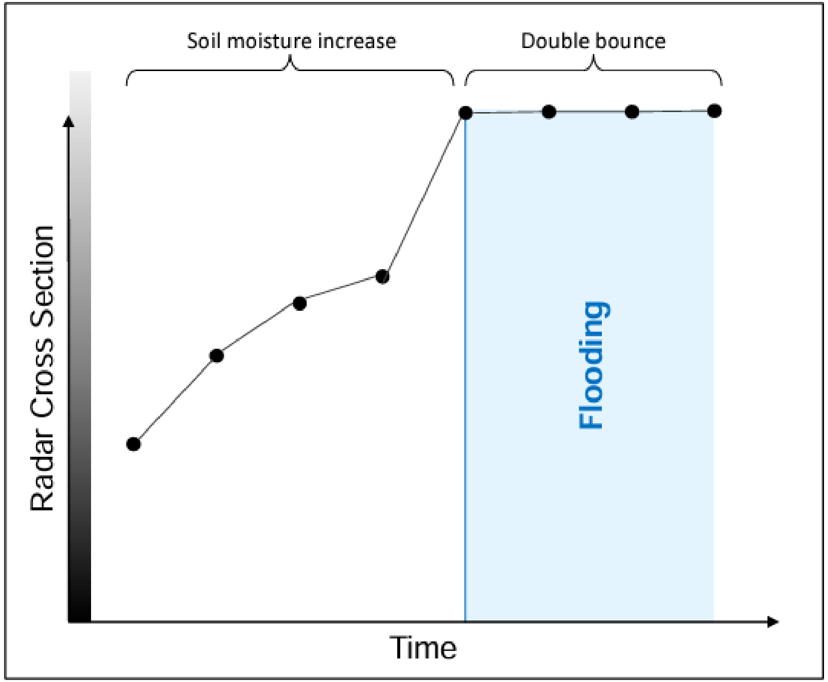

Flood Detection using SAR Data

2. Flooding under Vegetation Canopies

Example::

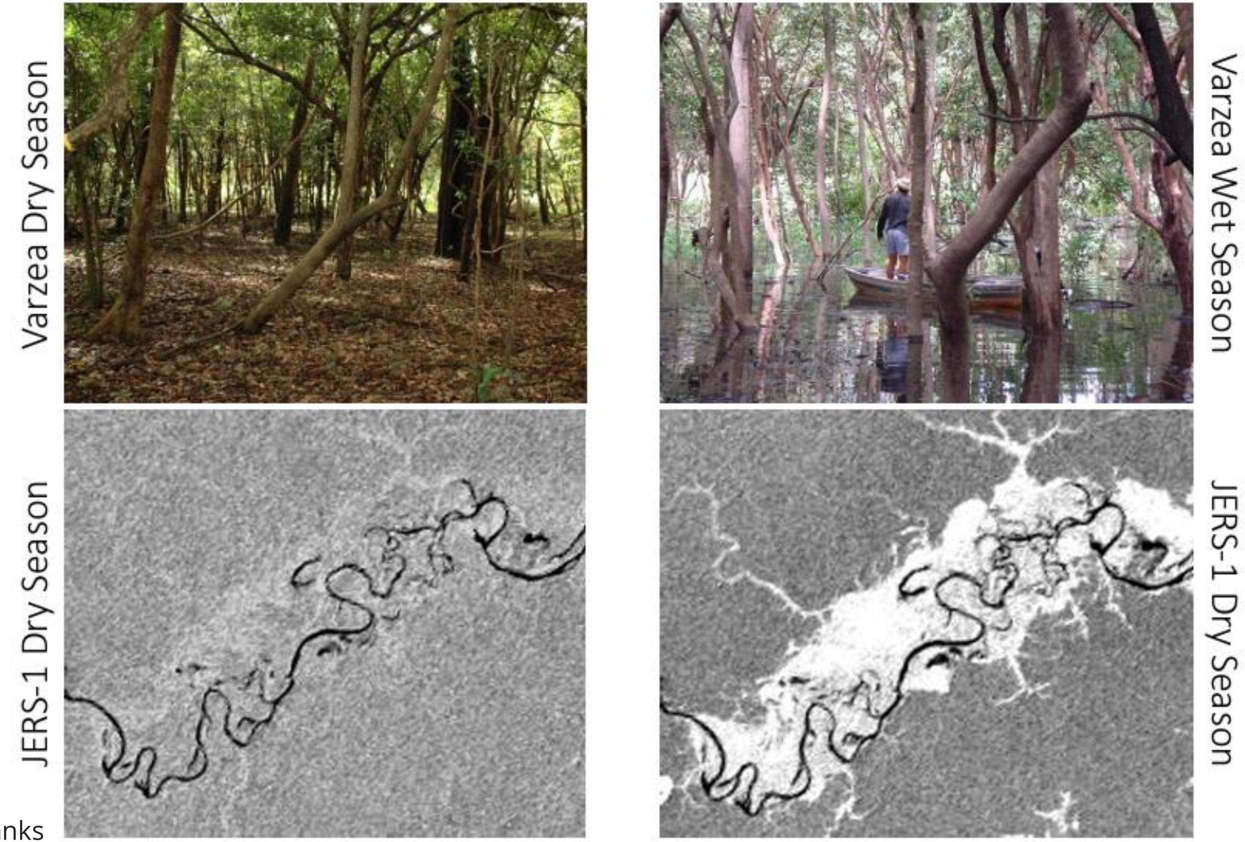

Flood Detection using SAR Data

3. Flooding in Crop lands

Mapping inundation in crop lands and wet meadows::

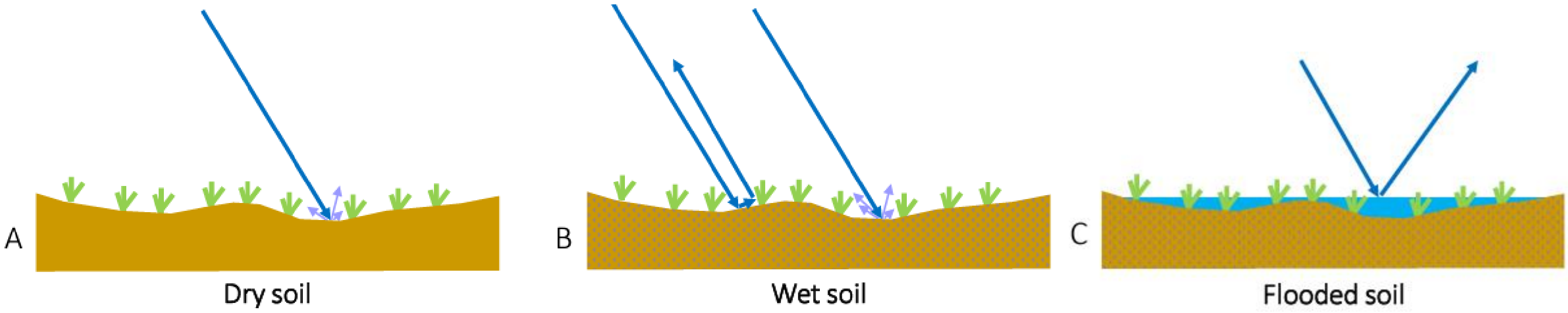

- A to B: The first backscatter increases with increasing soil moisture
- C: with increasing water level, backscatter becomes weaker with more specular reflection (scattering away from the sensor).

Flood Detection using SAR Data

3. Flooding in Crop lands

Relative SAR response in crop lands as precipitation increases::

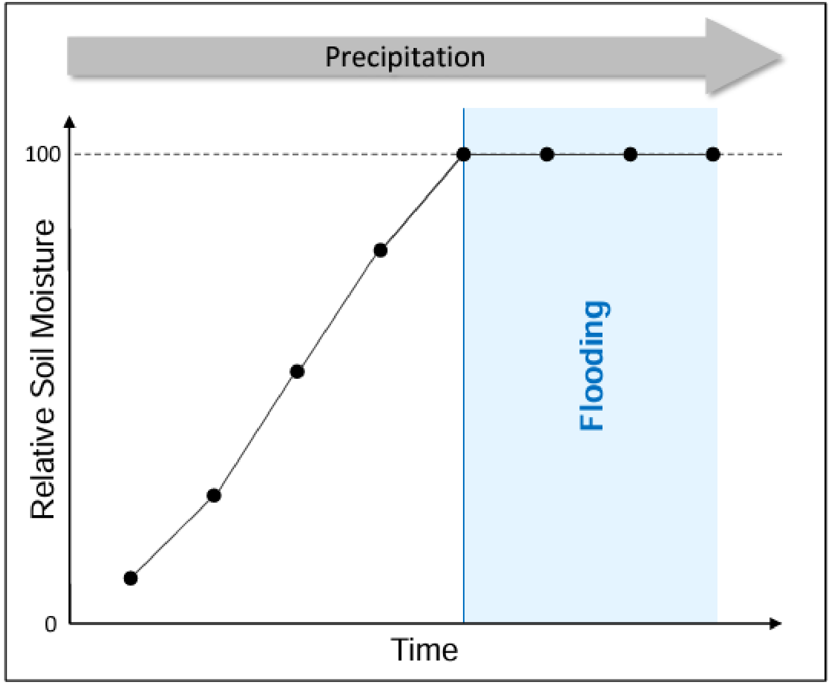

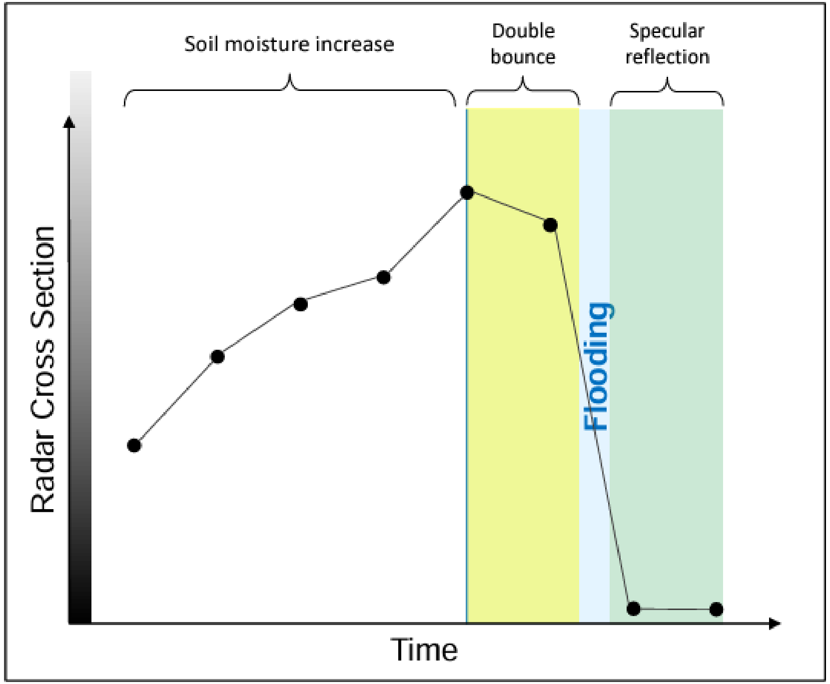

Flood Detection using SAR Data

Vegetation Inundation Mapping using SAR

SAR observations (especially at L-band) are established as a reliable tool for mapping vegetation inundation.

- C-band sensors limited performance in densely vegetated areas
- Existing L-band SARs have limited coverage to accurately capture spatial extent and temporal variations of inundation over wetlands.

JERS-1 L-band SAR (HH only) data showing inundation dynamics for 1 year (Jau River, Brazil)

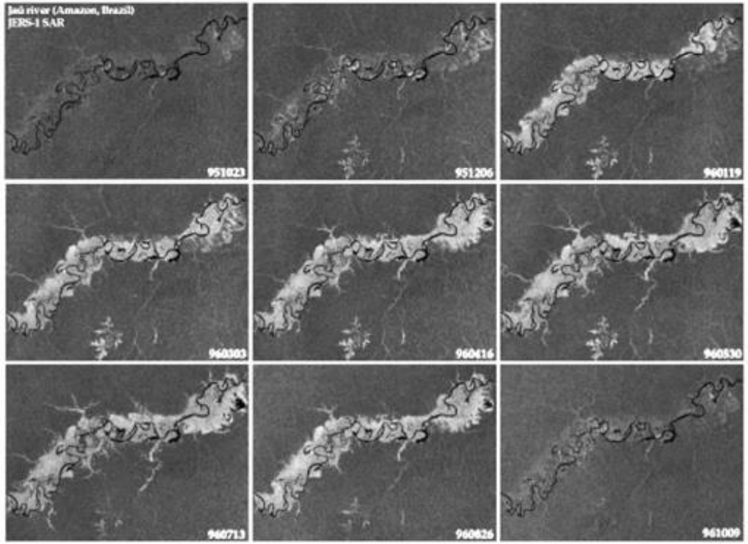

Rosenqvist et al, 1998.

Flood Detection using SAR Data

Surface Water Mapping Approaches from SAR Amplitude Images

One simple and common method for waterbody mapping is thresholding

- Backscatter below threshold classified as water body or inundated land
- Backscatter above threshold classified as dry land
- Thresholds derived from image histograms
- Results in binary mask (0 = land, 1 = water body)

Histogram of two Radarsat SAR images of the same region acquired under different incidence angles. Left: Radarsat S2 (23◦ incidence angle). Right: Radarsat S7 (45◦ incidence angle) (Solbø & Solheim, 2004)

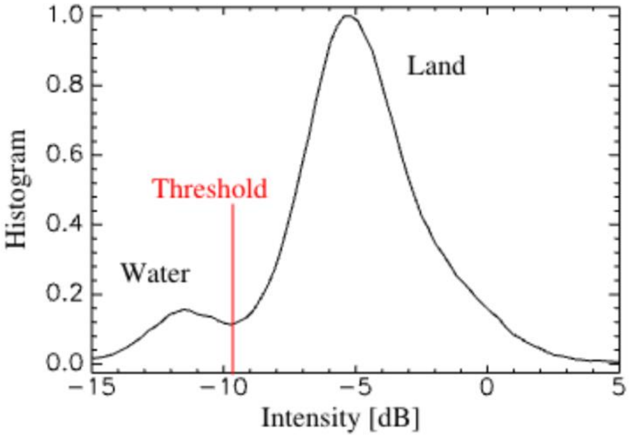

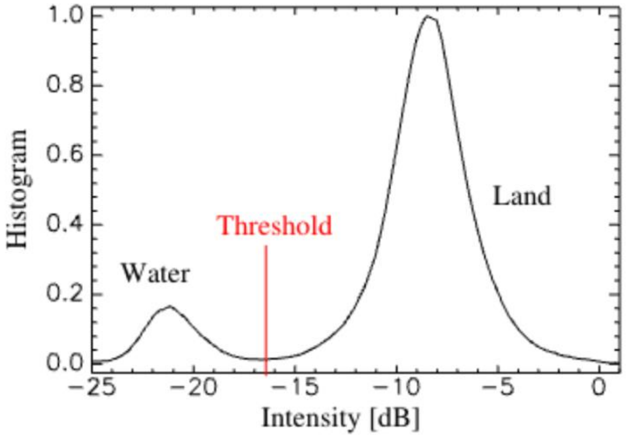

Flood Detection using SAR Data

Surface Water Mapping Approaches from SAR Amplitude Images

- Supervised image classification of multi-temporal SAR data
- Object-based classification of multi-temporal SAR data
- Mapping water bodies using active contours (”snakes“)
- Texture based classification
- Region growing algorithms
- Object-based classifications

- Single-frequency, single-polarization radar backscatter can be used

- Multi-temporal analysis requires:

– High-quality geometric correction and co-registration

– High-quality radiometric calibration and correction– Matching spatial resolution

Flood Detection using SAR Data

Surface Water Mapping Approaches from SAR Amplitude Images

Example of difference images and simple change detection for inundation mapping

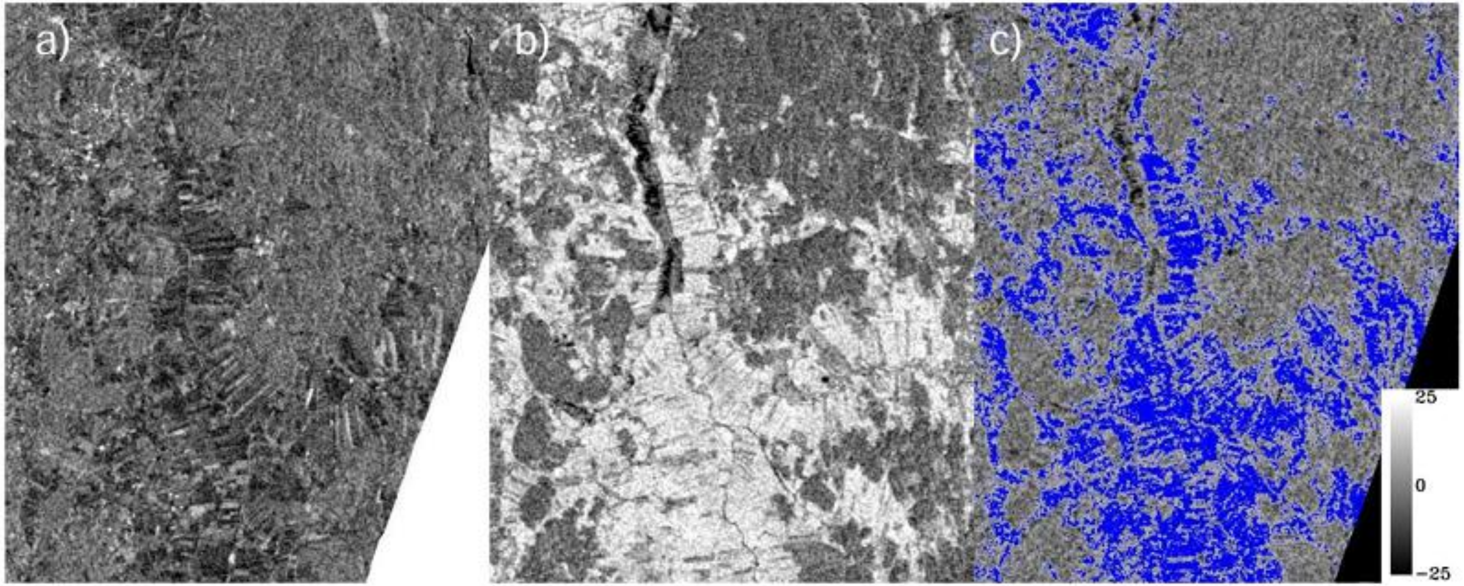

Fig.: Lapuanjoki area under normal (a) and flooded (b) conditions; difference image (c) shows flooded forest; ERS SAR Data (30m spatial resolution, acquired on 10th and 24th Jul 2001) (Solbø & Solheim, 2004)

Flood Detection using SAR Data

Surface Water Mapping Approaches from SAR Amplitude Images

Water as „dark“ areas with low backscatter

- Specular reflection
- Only a little backscatter directed back to sensor

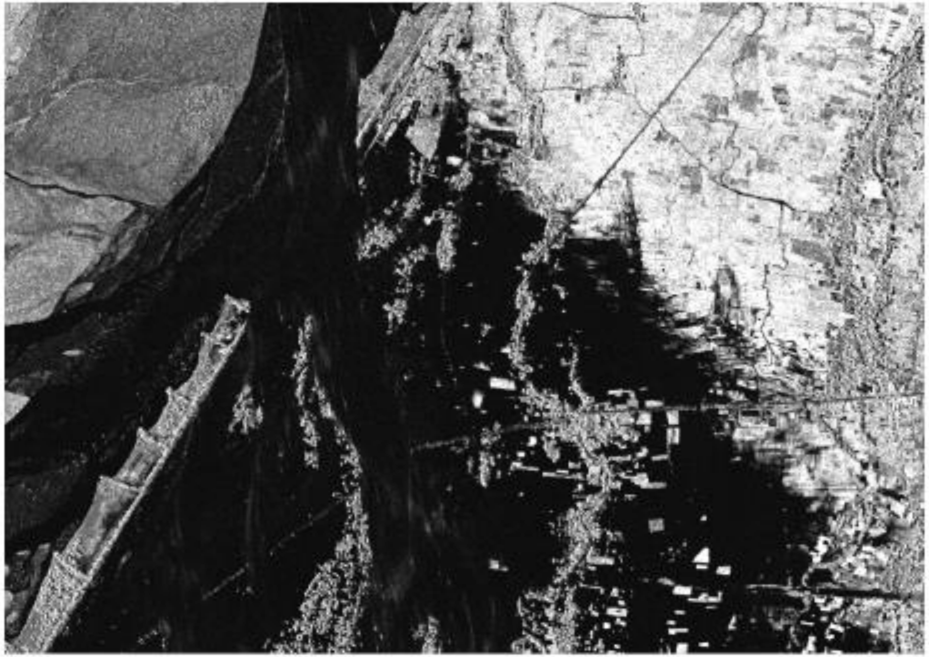

Nepal, TerraSAR-X, Spotlight, HH, 30.08.2008

Flood Detection using SAR Data

Water appearance – sensor-related effects

Incidence angle – steep vs. shallow

Steep incidence angles:
more reflection is directed back to the sensor

- higher backscatter
- land/water separation is more difficult

Shallow incidence angles:
mainly specular reflection away from the sensor

- Water is more likely to appear „black“

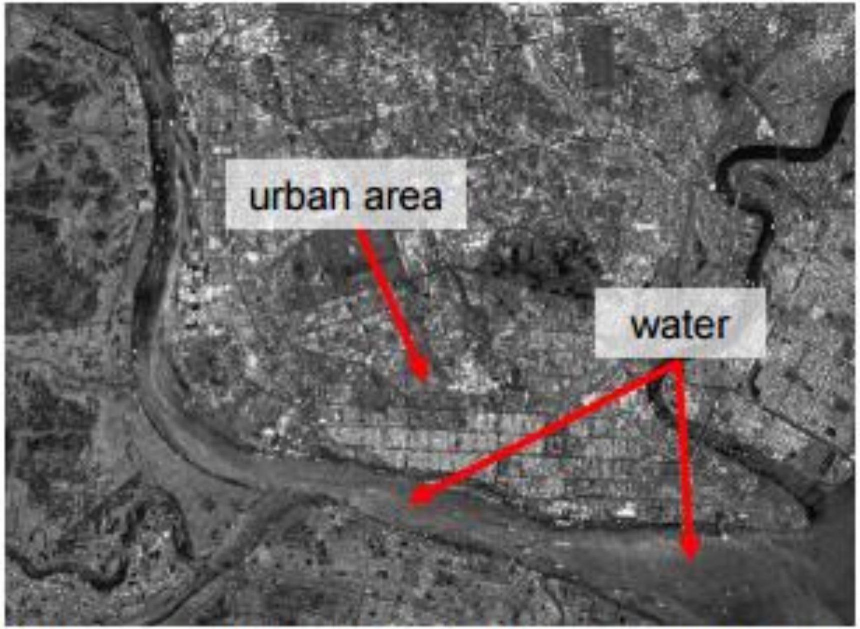

Myanmar, Spotlight, 09.05.08, Inc. Angle: 19°

Flood Detection using SAR Data

Water appearance – sensor-related effects

VV-polarization: More sensitive towards roughness at the water surface than HH-polarization

- increased backscatter
- land/water separation can become difficult during classification“

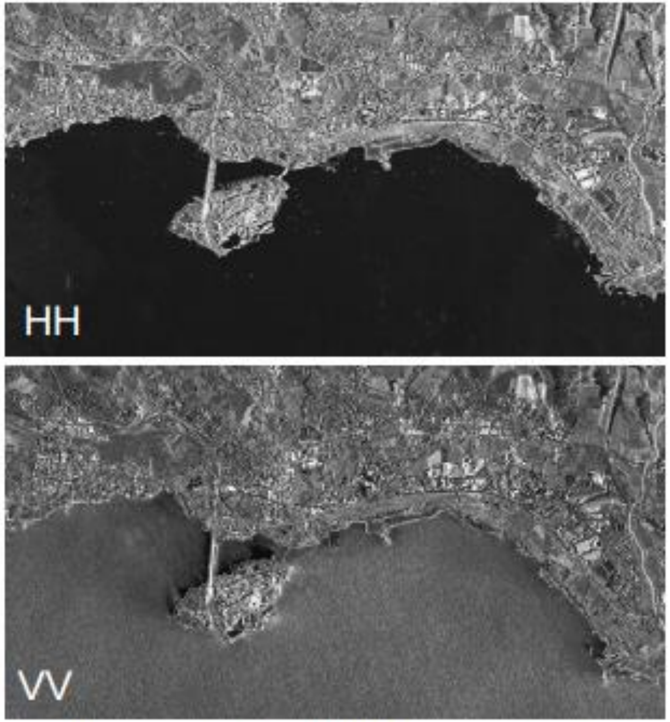

Lake Constance (GER), HighRes Spotlight

Flood Detection using SAR Data

Water appearance – sensor-related effects

SAR-Wavelenght – X-band (~3 cm) vs. L-band (~23 cm)

Differences in X- and L-band backscatter, particularly in moist areas and regions with flood waters beneath vegetation

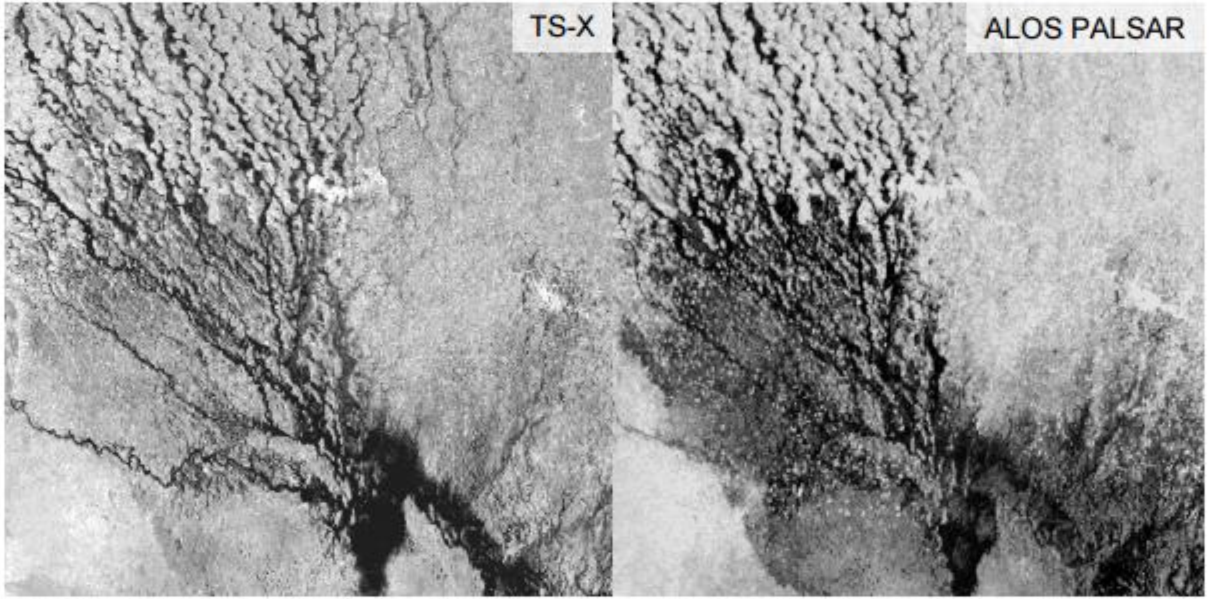

Flood Detection using SAR Data

Water appearance – wind / wave patterns

Separation of land surface and water bodies according to surface roughness

Problematic cases:

- Wind-induced waves
  - increased surface roughness
  - increased backscatter
  - possible confusion with land surface
- Sea waves: Refraction effects

Lake Ammersee (GER) at easterly winds, SM VV, 06.10.2007

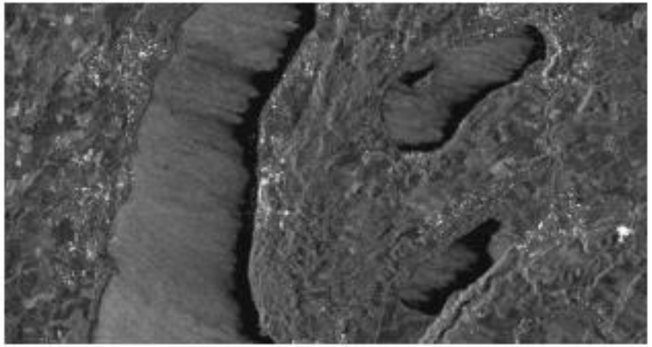

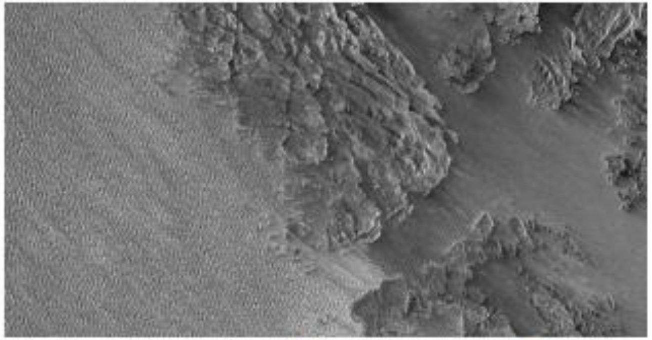

Bergen (NOR), StripMap, HH, 02.03.2008

Flood Detection using SAR Data

Objects with low backscatter values

Separation of land surface and water bodies according to surface Roughness

Potential for misclassification as water bodies/land surface

- Sand dunes (wave structures)
- Airstrips (smooth surface)

Walvis Bay (NAM), HR Spotlight, HH, 27.11.2007

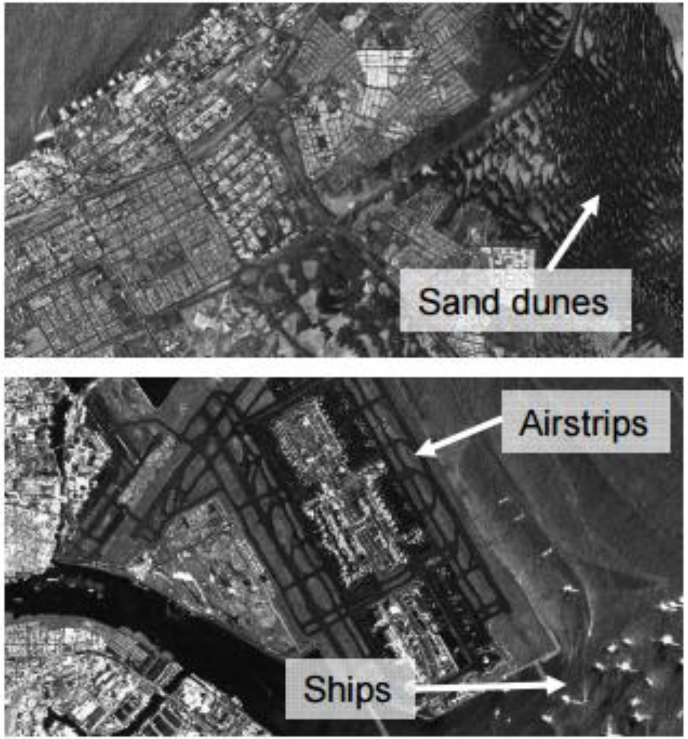

Tokio, Haneda Airport (JAP), SL VV, 12.11.2007

Flood Detection using SAR Data

Water bodies in mountainous terrain

Due to side-looking radar geometry no backscatter signal from areas behind mountain slopes (or buildings)

Possible confusion of water bodies and radar shadow areas

Lake Lucerne (Switzerland), SL VV, 10.10.2007

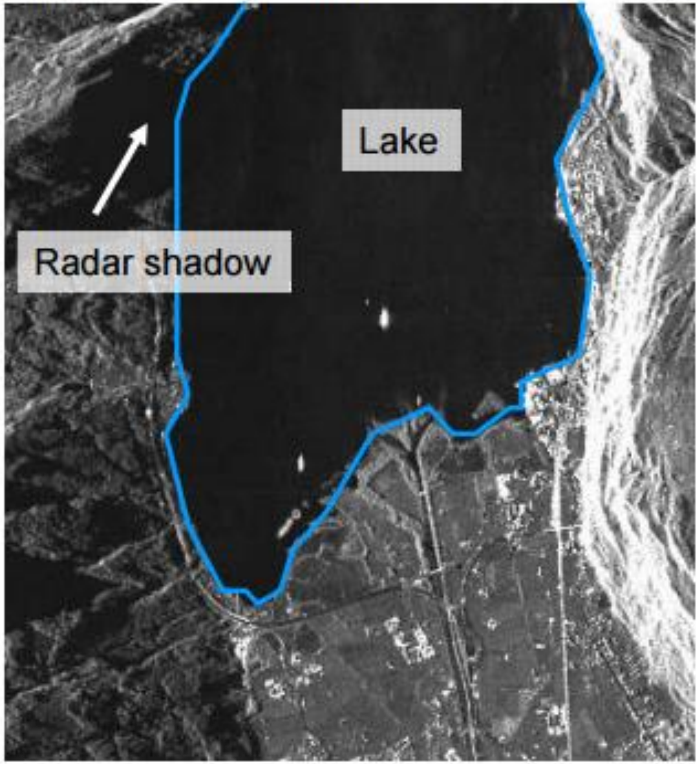

Flood Detection using SAR Data

Water bodies under forest

Water beneath the forest canopy

- high backscatter

Clarendon (Arkansas, USA), SM HH, 27.03.2008, spatial resolution 3.5 m

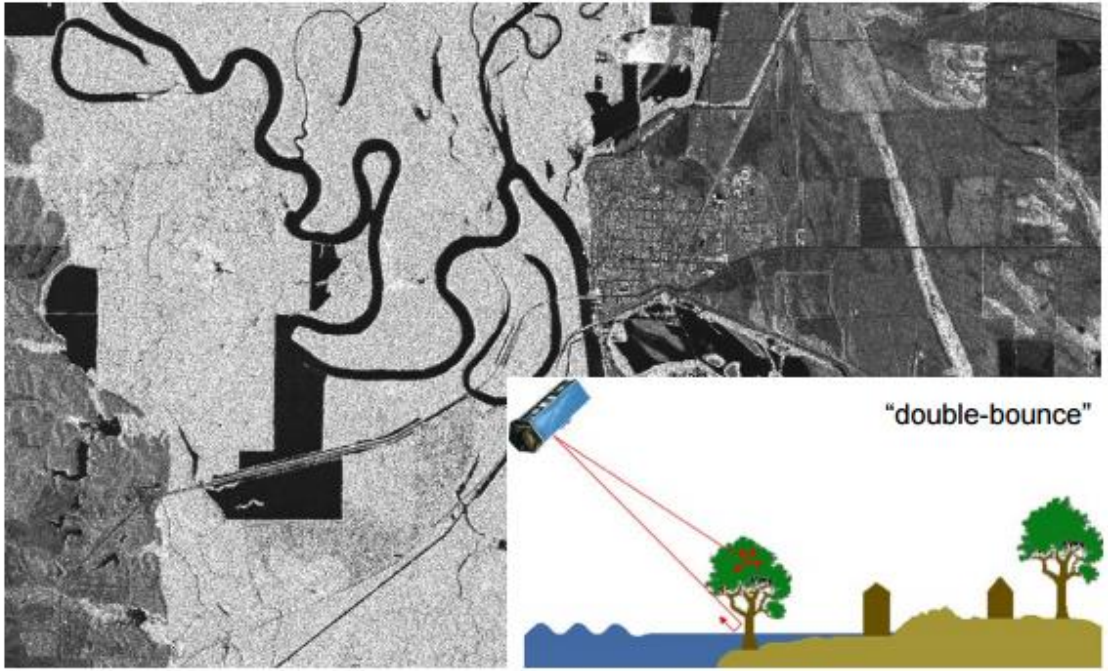

Flood Detection using SAR Data

Water bodies in urban areas

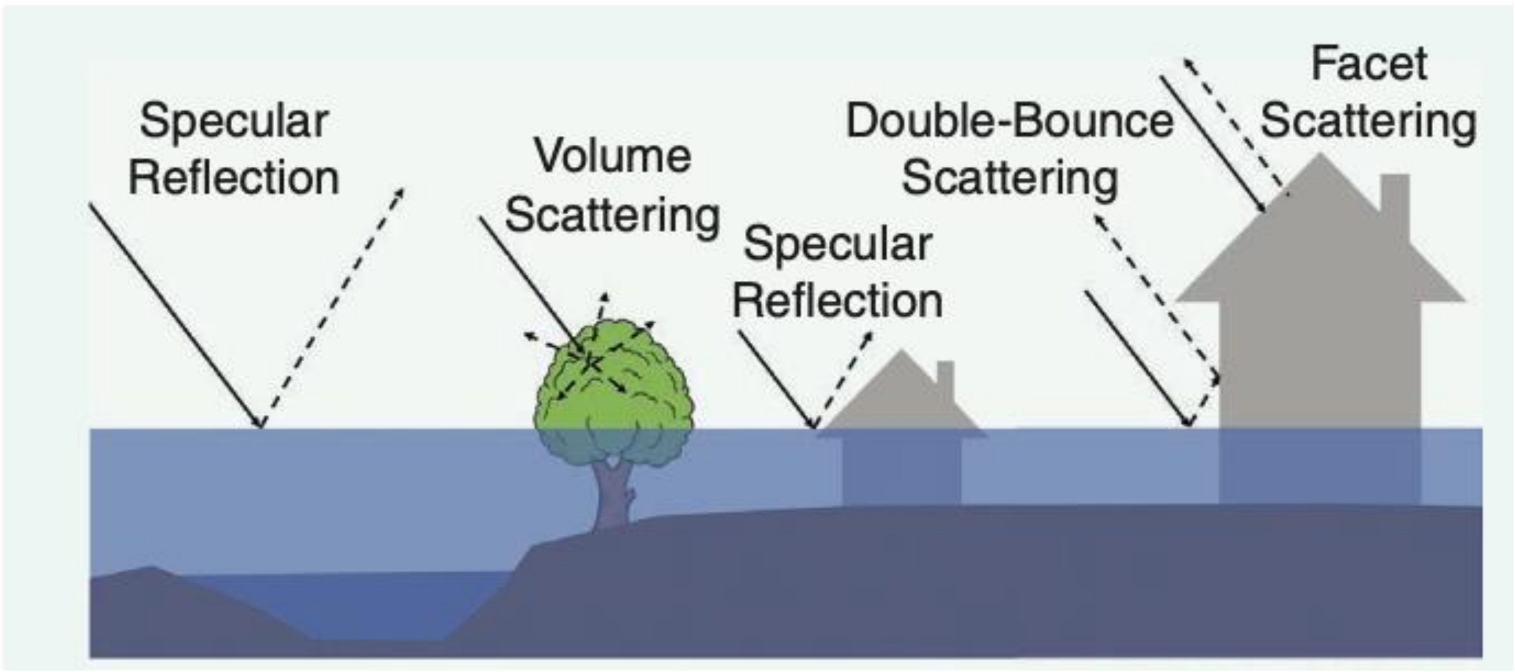

Jie Zhao et al., 2025. Urban Flood Mapping Using Satellite Synthetic Aperture Radar Data: A Review of Characteristics, Approaches and Datasets

Flood Detection using SAR Data

Water bodies in urban areas

Radar shadow from buildings

Discrimination between water and radar shadow difficult

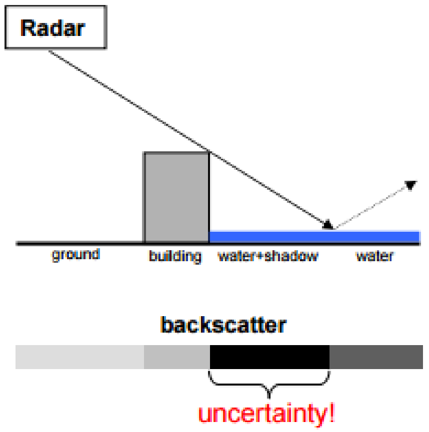

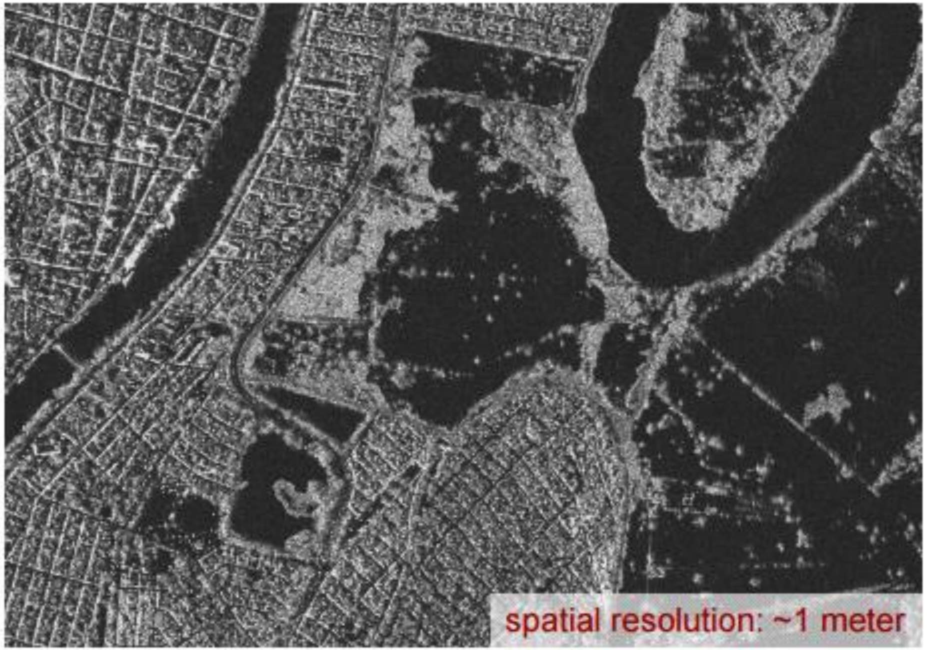

TerraSAR-X SpotLight-Mode - Mexico/Tabasco floods 11/2007

Flood Detection using SAR Data

Water bodies in urban areas

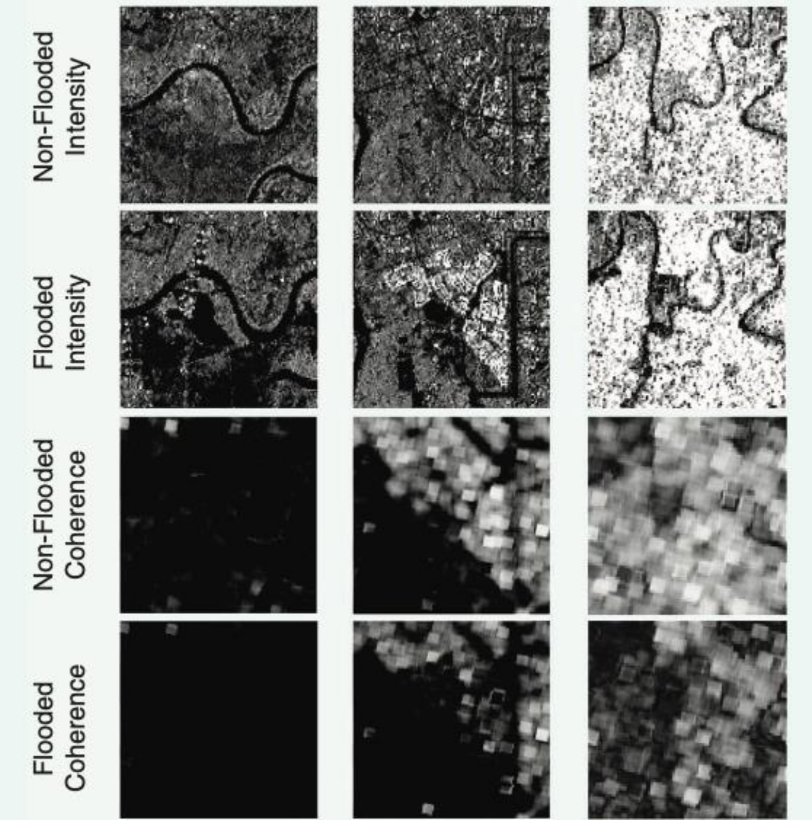

Jie Zhao et al., 2025. Urban Flood Mapping Using Satellite Synthetic Aperture Radar Data: A Review of Characteristics, Approaches and Datasets

Flood Detection using SAR Data

Flood mapping approaches for urban areas

- Visual inspection

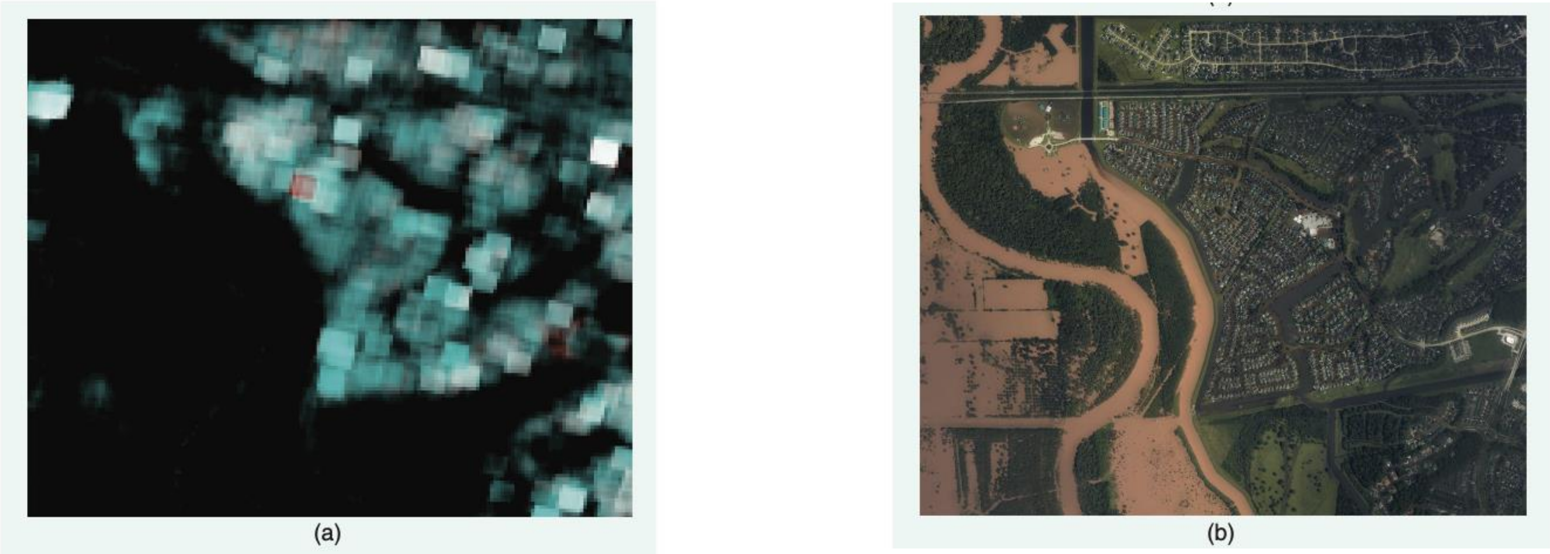

Example of visual inspection-based urban flood map- ping: (a) RGB composition of pre- and co-event InSAR coherence image in the Houston areas (R = co-event image, G = B = pre-event image); (b) optical image acquired after the flood event provided by National Oceanic and Atmospheric Administration.

Flood Detection using SAR Data

Flood mapping approaches for urban areas

- Coherence changes

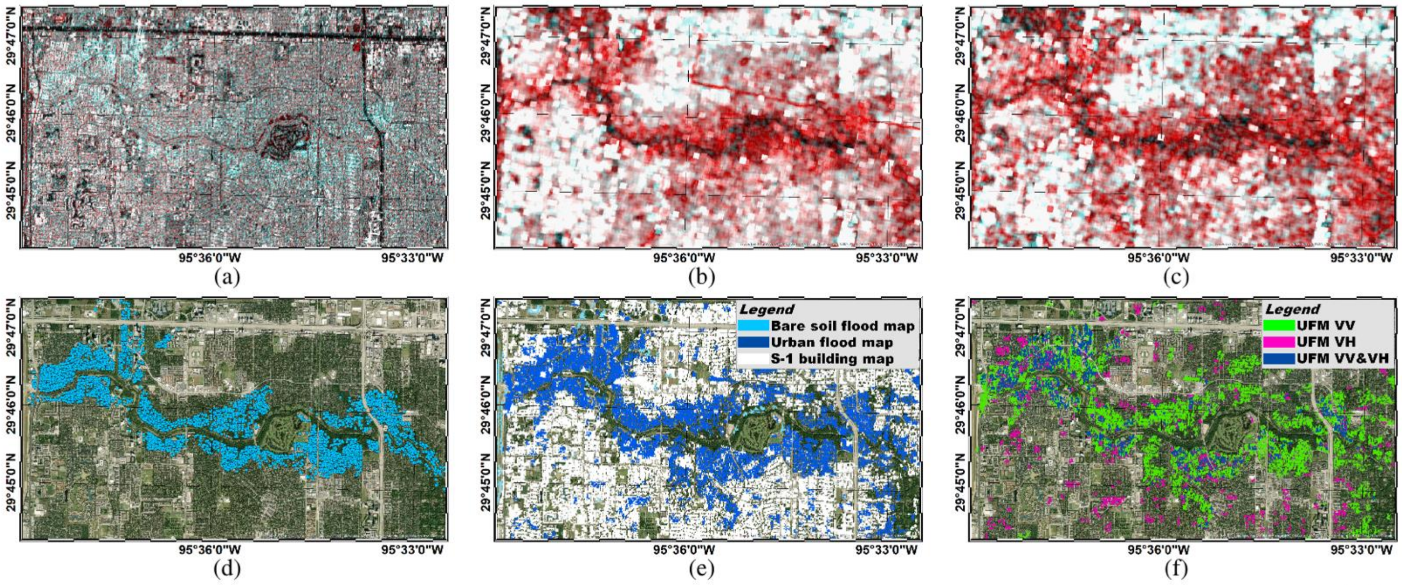

Fig. 5. AOI 1. (a) Intensity RGB composite: $R = 24/08/2017$, $B = G = 30/08/2017$. (b) VV and (c) VH InSAR ρ RGB composite: $R = \rho_{\text{pre}}^{18-24/08/2017}$, $B = G = \rho_{\text{co}}^{24-30/08/2017}$. (d) DG VHR imagery (31/08/2017) and crowd sourcing points of flooded buildings. (e) UFM (dark blue), flooded bare soil (light blue), nonflooded built-up areas (white). (f) VV–VH comparative UFM.

Ramona Pelich et al., 2022. Mapping Floods in Urban Areas From Dual-Polarization InSAR Coherence Data

Flood Detection using SAR Data

Flood mapping approaches for urban areas

- Coherence changes

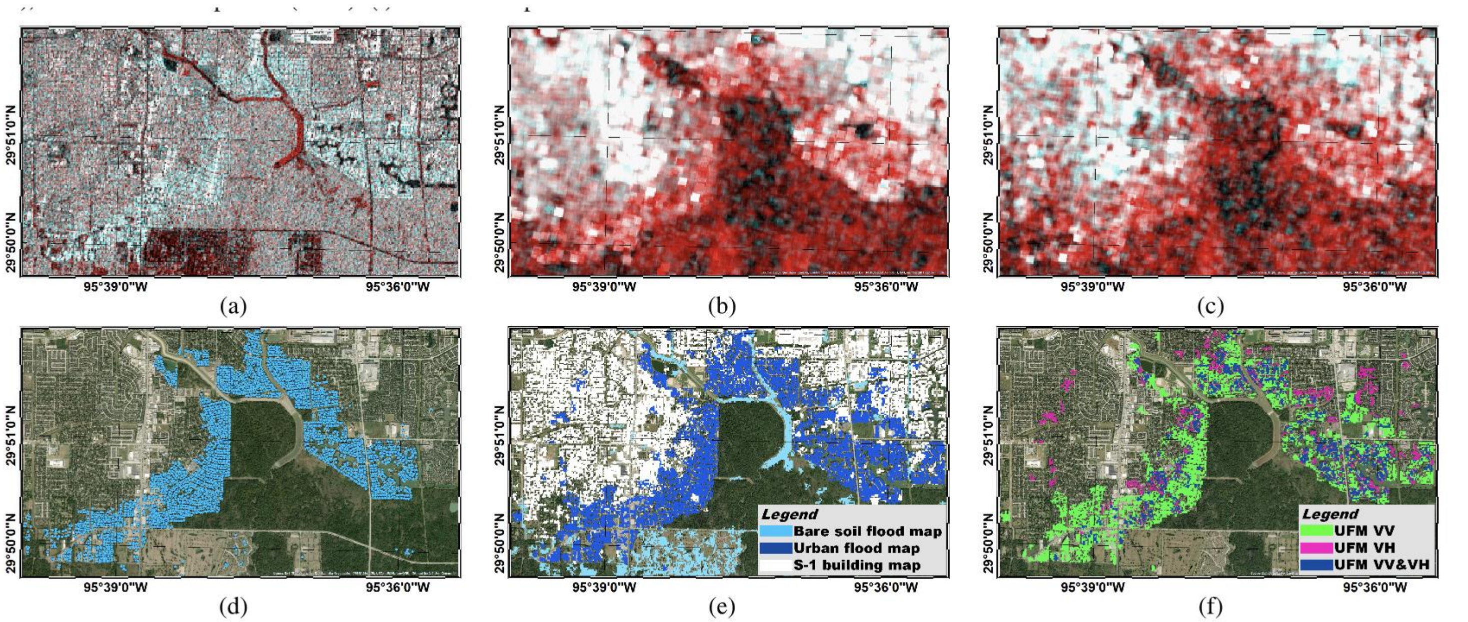

Fig. 6. AOI 2. (a) Intensity RGB composite: $R = 24/08/2017$, $B = G = 30/08/2017$. (b) VV and (c) VH InSAR ρ RGB composite: $R = \rho_{\text{pre}}^{18-24/08/2017}$, $B = G = \rho_{\text{co}}^{24-30/08/2017}$. (d) DG VHR imagery (31/08/2017) and crowd sourcing points of flooded buildings. (e) UFM (dark blue), flooded bare soil (light blue), nonflooded built-up areas (white). (f) VV–VH comparative UFM.

Ramona Pelich et al., 2022. Mapping Floods in Urban Areas From Dual-Polarization InSAR Coherence Data

THANK YOU

Geoinformatics Center, Asian Institute of Technology